Front. Electr. Electron. Eng. 2012, 7(4): 438–446
DOI 10.1007/s11460-012-0212-0

RESEARCH ARTICLE

M. MADHESWARAN, C. NAGARAJAN

DSP based fuzzy controller for series parallel resonant converter

Abstract In this paper, digital signal processor (DSP) based fuzzy controller for series parallel resonant converter (SPRC) has been estimated, and the performance of the converter is analyzed by using state space model. The method to predict the steady-state and dynamic performance of the converter with load independent operation has been presented. The proposed converter has been analyzed with the closed-loop and open-loop conditions. The simple form of transfer function for SPRC is developed, and it is used to analyze the stability of the converter with closed-loop operation. The stability analysis of the converter is carried out by using frequency response plan. The fuzzy controller regulates the output voltage with change supply voltage and load disturbance. The controller performance of inductance capacitance inductance – T network (LCL-T) SPRC is compared with inductance inductance capacitance – T network (LLC-T) SPRC through simulation and experimental studies using TMS320F2407 processor.

Keywords power electronics, DC-DC power converters, fuzzy control, system analysis and design

1 Introduction

Recently for medium and high power applications at high voltages, resonant converters have been found a realistic solution. The research in this field has been shown more interest by many researchers in developing the load independent converters using various concepts. They are gaining extensive popularity among their excellent performance like output voltage with negligible total harmonic distraction (THD), reduced rippled and regulated output voltage, reduced voltage stress, and low electro magnetic interference (EMI) emission. It has been suggested to design resonant converter with three reactive components for better regulation. To overcome the above limitations, the series parallel resonant converter (SPRC) is found to be reliable due to various inherent advantages. Among all the topologies of the resonant converters, the SPRC shares the advantages of both the pure series converter and pure parallel converters. The inductance capacitance inductance (LCL) tank circuit based DC-DC resonant converter has been experimentally demonstrated and reported by many researchers [1,2].

Borage et al. [3] have demonstrated an LCL-T half bridge resonant converter with clamp diodes, in which the output voltage of constant current power supply increases linearly. Therefore, a constant-voltage limit must be incorporated in the converter. To get these operations, the clamp diode is required. The feedback control circuit has not been considered. Later, Borage et al. [4] have demonstrated the LCL-T resonant converter with constant current supply operated at resonant frequency. The converter operated at fixed resonant frequency, and it was analyzed by using state space approach. Borage et al. [5] have demonstrated the characteristics of LCL-T resonant converter using asymmetrical duty cycle (ADC). Belaguli et al. [6] have experimentally demonstrated LCL tank circuit with independent load when operated at resonant frequency, making it attractive for application as a constant voltage (CV) power supply. It has been found from the literature that the LCL tank circuit connected in series-parallel with the load and operated in above resonant frequency improves the load efficiency and independent operation. Mattavelli et al. [7] have described the fuzzy logic control (FLC) for DC-DC converter. This control technique relies on the human capability to understand the system's behavior and is based on qualitative control rules. The FLC approach with same

Received July 25, 2012; accepted October 8, 2012

M. MADHESWARAN, C. NAGARAJAN (✉)
Centre for Advanced Research, Muthayammal Engineering College, Rasipuram-637408, Tamilnadu, India
E-mail: nagaraj2k1@gmail.com

control rules can be applied to several DC-DC converters. However, some scale factors must be tuned according to converter topology and parameters. The authors used and demonstrated the control technique for buck-boost converter. Correa et al. [8] have demonstrated a DC/AC series resonant converter with fixed load with considering fuzzy control approaches.

Lakshminarasamma et al. [9] have demonstrated active clamp zero voltage switching (ZVS) DC-DC converter. The steady-state stability analysis was presented for ZVS buck converter. There is no possibility of load independent operation. The converter operates at duty cycle > 0.5, above its operation the converter fails to instability. Arun et al. [10] demonstrated the ZVS LCL push-pull converter with closed-loop operation using proportional-integral (PI) controller. Resonant topology like LCL and LLC resonant converter are compared with open-loop and closed-loop. Here, the load variation and load independent operation were not presented, and there was no static and dynamic analysis. Later, Foster et al. [11] have demonstrated CLL half bridge resonant converter with open-loop operation. The AC equivalent circuit analysis and fundamental mode approximation (FMA) analysis were derived, which are used to model the converter and compared to each other. The evaluation of static and dynamic performance was not provided.

Later, Sivakumaran et al. [12] have developed a CLC SPRC using FLC for load regulation and line regulation. The performance of the controller has been evaluated and it was found that the load independent operation may not be possible. The FLC based ZVS quasi-resonant converter has been demonstrated in Refs. [13–16]. The load independent operation was not realized and power handling capacity of the converter is found to be poor. Nagarajan et al. [17] have simulated an LCL-T SPRC by using FLC and PID controller. The performance of the controller has been found to be better when the fuzzy controller has been considered. The harmonic spectrum and dynamic analysis for resistive inductive voltage source RLE load are presented.

It is clear from the above literatures that the output voltage regulation of the converter against load and supply voltage fluctuations has important role in designing high-density power supplies. The LCL-T SPRC is expected to have the speed of response, voltage regulation, and better load independent operation. Keep the above facts in view, the LCL-T SPRC has been modeled and analyzed for estimating various responses. The closed-loop state space model has been derived and simulated using MATLAB/Simulink. The steady-state stability analysis of the converter is presented. Prototype of 300 W, 100 kHz LCL-T SPRC and LLC-T SPRC are implemented and the experiment results are compared with the simulation results. The simulation results agree with the experimental results.

2 Modified SPRC

The circuit diagram of SPRC is shown in Fig. 1. The first stage of the converter is to convert the DC voltage to a high frequency AC voltage. The second stage of the converter is to convert the AC power to DC power by suitable high frequency rectifier and filter circuit. Power from the resonant circuit is taken either through a transformer in series with the resonant circuit or series in the capacitor comprising the resonant circuit. In both the cases, the high frequency feature of the link allows the use of a high frequency transformer to provide voltage transformation and ohmic isolation between the DC source and the load.

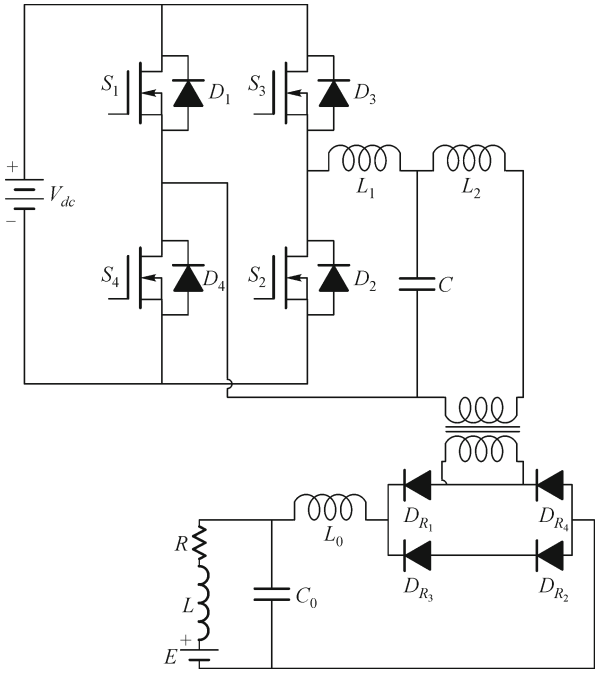

Fig. 1 Series parallel resonant converter

3 Stability analysis of SPRC using state space technique

3.1 State space model for LCL-T SPRC

The equivalent circuit of LCL-T SPRC is shown in Fig. 2. The mathematical model using state space technique can be obtained by assuming all the components to be ideal.

The transfer function for the LCL-T SPRC is derived from Fig. 2:

$$\frac{V_0(s)}{V_i(s)} = \frac{Z_L}{L_1L_2Cs^3 + L_1Z_LCs^2 + (L_1 + L_2)s + Z_L}. \quad (1)$$

The differential equations of linear network can be written in the form:

$$\dot{x}(t) = Ax(t) + Bu(t), \quad (2)$$

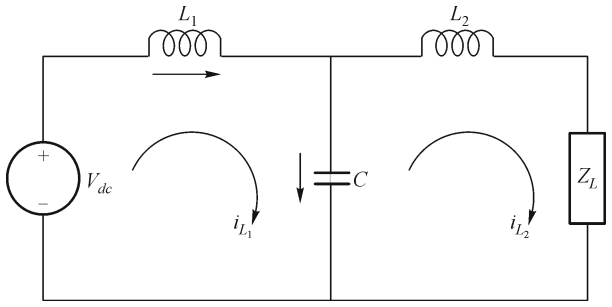

Fig. 2 Equivalent circuit model of LCL-T SPRC

$$\dot{y}(t) = Cx(t) + Du(t). \tag{3}$$

This system of first order differential equation is known as the state equation of the system. $x(t)$ is the state vector and $u(t)$ is the input vector. The second equation is referred to as the output equation. A is called the state matrix, B the input matrix, C the output matrix, and D the direct transition matrix. One advantage of the state space method is that the form lends itself easily to the digital or analog computer methods of solution. The state space methods can be easily extended to analysis of nonlinear systems. The state space model for LCL-T SPRC can be derived from Eq. (1) and can be written as

$$\frac{Y_0(s)}{u_i(s)} = \frac{Z_L}{L_1L_2Cs^3 + L_1Z_LCs^2 + (L_1 + L_2)s + Z_L}. \tag{4}$$

Taking inverse Laplace transform (4), the state space equations are

$$\dot{X}_1 = x_2, \tag{5}$$

$$\dot{X}_2 = x_3, \tag{6}$$

$$\dot{X}_3 = \frac{-Z_L}{CL_1L_2}x_1 - \left(\frac{L_1}{CL_1L_2} + \frac{L_2}{CL_1L_2}\right)x_2 - \frac{L_1Z_L}{L_1L_2}x_3 + \frac{Z_L}{CL_1L_2}u_i(s). \tag{7}$$

The state space model for LCL-T SPRC is

$$\begin{bmatrix}\dot{X}_1\\ \dot{X}_2\\ \dot{X}_3\end{bmatrix} = \begin{bmatrix}0 & 1 & 0\\ 0 & 0 & 1\\ \dfrac{-Z_L}{CL_1L_2} & \dfrac{-1}{CL_2} - \dfrac{1}{CL_1} & \dfrac{-Z_L}{L_2}\end{bmatrix}\begin{bmatrix}x_1\\ x_2\\ x_3\end{bmatrix} + \begin{bmatrix}0\\ 0\\ \dfrac{Z_L}{CL_1L_2}\end{bmatrix}[u_i(s)]. \tag{8}$$

The output equation is

$$y_0 = [\,1 \quad 0 \quad 0\,]\begin{bmatrix}x_1\\ x_2\\ x_3\end{bmatrix}. \tag{9}$$

3.2 State space model for LLC-T SPRC

The equivalent circuit of LLC-T SPRC is shown in Fig. 3. The state space equation can be derived from the transfer function (10).

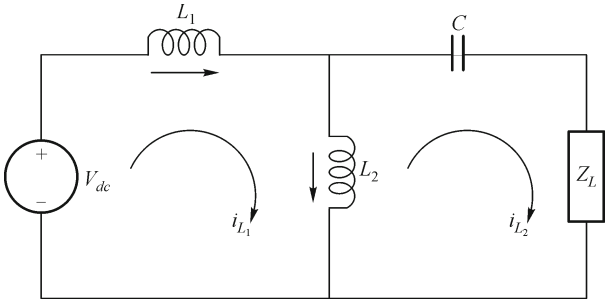

Fig. 3 Equivalent circuit model for LLC-T SPRC

The transfer function for the LLC-T SPRC is given below from Fig. 3:

$$\frac{Y_0(s)}{u_i(s)} = \frac{Z_3Z_L}{Z_1Z_2 + Z_1Z_3 + Z_1Z_L + Z_2Z_3 + Z_3Z_L}, \tag{10}$$

$$\frac{Y_0(s)}{u_i(s)} = \frac{L_2Z_Ls}{\dfrac{(L_1 + L_2)}{C} + L_1L_2s^2 + [L_1Z_L + L_2Z_L]s}. \tag{11}$$

Taking inverse Laplace transform in Eq. (11), the state space equations are

$$\dot{X}_1 = x_2, \tag{12}$$

$$\dot{X}_2 = -\frac{(L_1 + L_2)}{CL_1L_2}x_1 - \frac{(L_1Z_L + L_2Z_L)}{L_1L_2}x_2 + \frac{Z_L}{L_2}u_i(s). \tag{13}$$

In above, the state space equations are written in matrix form. The state space model for LLC-T SPRC is

$$\begin{bmatrix}\dot{X}_1\\ \dot{X}_2\end{bmatrix} = \begin{bmatrix}0 & 1\\ -\dfrac{L_1 + L_2}{CL_1L_2} & -\dfrac{(L_1Z_L + L_2Z_L)}{L_1L_2}\end{bmatrix}\begin{bmatrix}x_1\\ x_2\end{bmatrix} + \begin{bmatrix}0\\ \dfrac{Z_L}{L_1}\end{bmatrix}[u_i(s)]. \tag{14}$$

The output equation is

$$y_0 = \begin{bmatrix} 1 & 0 \end{bmatrix} \begin{bmatrix} x_1 \\ x_2 \end{bmatrix}. \quad (15)$$

4 Results and discussion

4.1 Fuzzy logic control (FLC)

Fuzzy control involves three stages: fuzzification, inference or rule evaluation, and defuzzification. SPRC is modeled using MATLAB software. Fuzzy control is developed using the fuzzy toolbox. The fuzzy variables "*e*", "*ce*", and "Δu" are described by triangular membership functions. Table 1 shows the fuzzy rule base that is created in the present work based on intuitive reasoning and experience. The linguistic labels are divided into seven groups:

- NH: negative high,
- N: negative,
- NL: negative low,
- Z: zero,
- PL: positive low,
- P: positive,
- PH: positive high.

It can be inferred that the output voltage is far from the reference value; then, the change of switching frequency (Δu) must be large so as to bring the output to the reference value quickly. The output voltage approaches the reference value; and then, a small change of switching frequency is necessary. If the output voltage is near the reference value and is approaching the reference value rapidly, then the frequency must be kept constant so as to prevent overshoot. It is also seen that if the output voltage changes even after reaching the reference value, then the change of frequency must be changed by a small amount to prevent the output from moving away.

Table 1 Fuzzy rules

change in error (*ce*)	error (*e*)						
	NH	N	NS	Z	PL	P	PH
NB	NH	NH	NH	NH	N	NL	Z
N	NH	NH	N	N	NL	Z	PL
NL	NH	N	NL	NL	Z	PL	P
Z	NH	N	NL	Z	PL	P	PH
PL	N	NL	Z	PL	PL	P	PH
P	NL	Z	PL	P	P	PH	PH
PH	Z	PL	P	PH	PH	PH	PH

4.2 Simulation results

The designed procedure of the converter was presented in Ref. [17]. The closed-loop simulation using FLC is carried out using MATLAB/Simulink software. Depending on error and the change in error, the value of change of switching frequency is calculated. The fuzzy set parameters instruction and function blocks available in MATLAB are used to update the new switching frequency of the pulse generators. The entire system is simulated with a switching frequency of 100 kHz.

The LCL-T SPRC and LLC-T SPRC have been simulated using MATLAB/Simulink toolbox. The fuzzy controller has been designed, and simulated wave forms of resonant voltage, resonant current, and output voltage are shown in below figures. The fuzzy controller performance is compared with the resonant topologies.

4.2.1 LLC-T SPRC using FLC

The fuzzy controller has been designed, and simulated wave forms of resonant voltage, resonant current, and output voltage are shown in Figs. 4–6. The slight drop in the resonant characteristics is due to the increase in conduction losses in the bridge inverter and resonant network. It is observed that the voltage and current are not match with the phase of the resonance. It is clearly seen

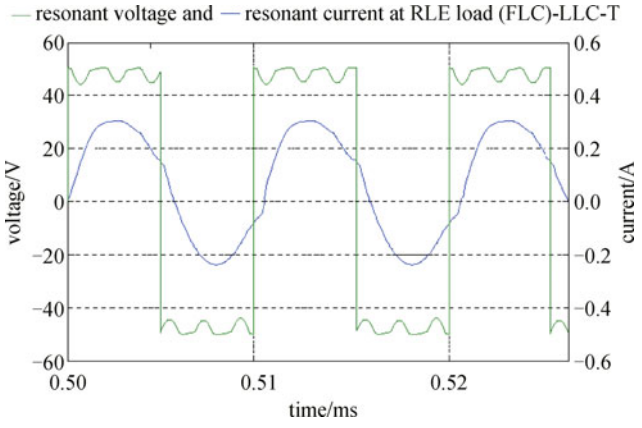

Fig. 4 Resonant current and resonant voltage for V_R = 100 V

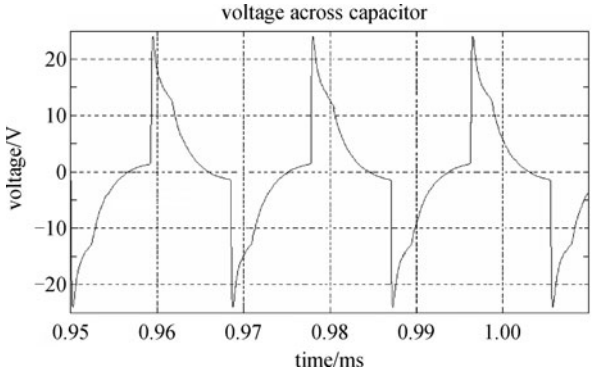

Fig. 5 Voltages across parallel capacitor (*C*)

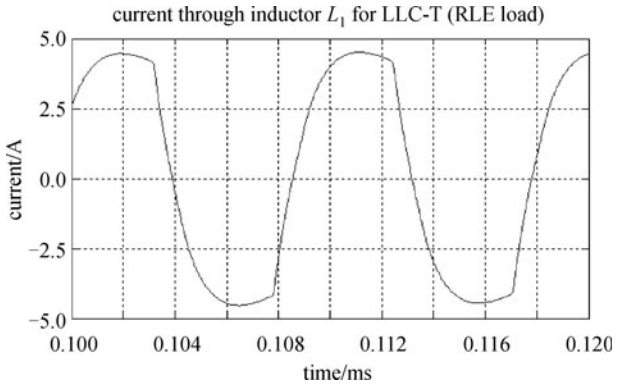

Fig. 6 Current through inductance L_1 (LLC-T SPRC with FLC fed RLE load)

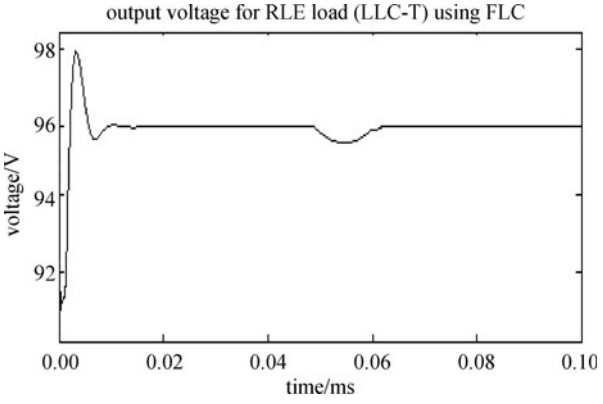

Fig. 8 Output voltage for step change in load at $t = 0.05$ ms

from Fig. 4 that the resonant voltage and current contain harmonic.

The voltage wave form for capacitor is shown in Fig. 5. It can be seen from Fig. 5 that the capacitor voltage is not zero during the interval time.

The current are measured through inductor L_1, and the current through inductor L_1 is shown in Fig. 6.

Figure 7 shows the simulated output voltage with step change supply at $t = 0.05$ ms. The output voltage with load disturbance is show in Fig. 8. It is observed that the settling time in FLC is 0.01 ms. The steady-state error for LLC-T SPRC is 0.004 V. The result is justified that the settling time of output voltage of LLC-T SPRC is higher than that of LCL-T SPRC.

4.2.2 LCL-T SPRC using FLC

The resonant current and resonant voltage were estimated and shown in Fig. 9. The overshoot and settling time are less than other converter, and the response is oscillatory. It is seen that the settling time of output voltage is more than that of the settling time in LLC-T. It is clearly shown that the inverter output is pure square wave without any harmonics and with resonance frequency.

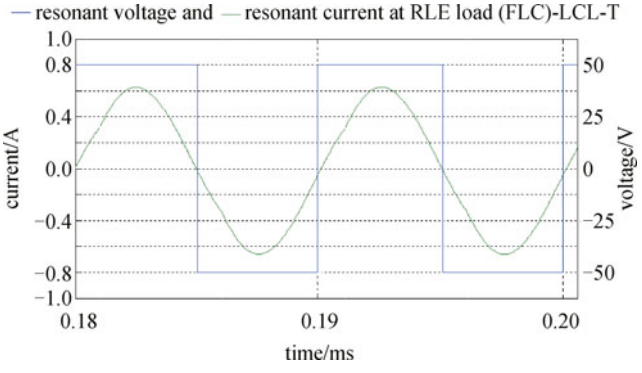

Fig. 9 Resonant current and resonant voltage for $V_R = 100$ V (LCL-T SPRC with FLC fed RLE load)

It can be seen from Fig. 9 that after an initial transient, the resonant voltage and resonant current are accuracy well, which show a good tracking performance of the controller. The resonant current contains low harmonic and it presents a good sinusoidal shape.

Figure 10 shows the voltage across parallel capacitor

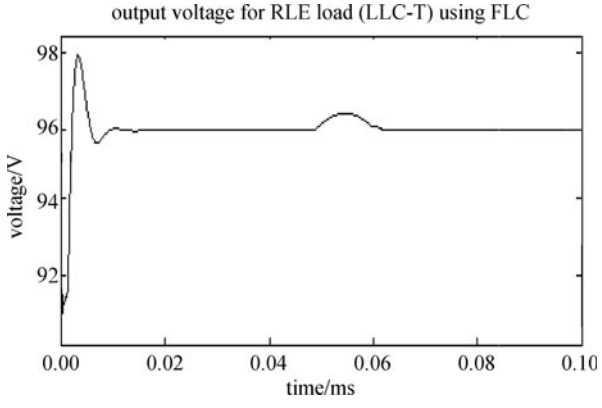

Fig. 7 Output voltage for step change in supply at $t = 0.05$ ms

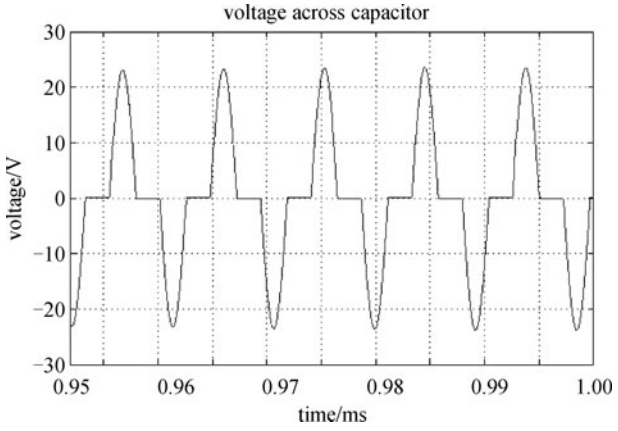

Fig. 10 Voltages across parallel capacitor (C) (LCL-T SPRC with FLC fed RLE load)

waveform at steady-state. Figure 11 shows the inductor current L_1 and the current is quite sinusoidal as the converter operates in the resonance frequency. It is almost sinusoidal because the operating frequency virtually matches with the resonance frequency. In this condition, the circuit has a good margin for zero voltage switching operation, providing good response, while the almost sinusoidal current waveform just allows for an extremely low EMI generation.

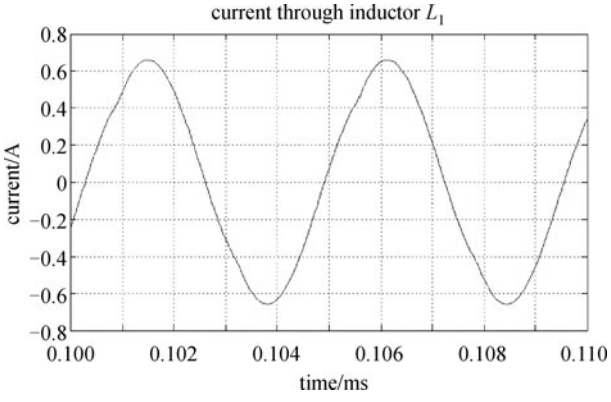

Fig. 11 Current through inductance L_1 (LCL-T SPRC with FLC fed RLE load)

Figure 12 clearly shows the simulated output voltage with step change load at t = 0.05 ms. The output voltage with load disturbance is show in Fig. 13. The fuzzy logic controller shows the regulate output voltage with less settling time that is nearly 0.01 ms. Also, the overshoot in output voltage is reduced to 1%. The settling time of the LLC-T SPRC is high comparing to LCL-T SPRC.

The performance of resonant topologies like LCL-T SPRC and LLC-T SPRC responses have been estimated and provided in Table 2. It is seen that the fuzzy logic based closed-loop controller in LCL-T SPRC provides better settling time. This ensures that the system can be controlled effectively with feedback.

It is clear from the above table that the peak overshoot is eliminated and the settling time is much lower with the fuzzy control strategy in LCL-T SPRC. The measurement noise is highly suppressed. It is also obvious that the settling times of different resonant topologies have been compared and concluded that FLC has got better performance in LCL-T SPRC.

4.3 Stability analysis

Frequency response plots for LLC-T SPRC are shown in Fig. 14. The plots are drawn by using the state space model Eqs. (3) and (4). It clearly shows that the LLC-T converter is unstable, the phase margin (α) and the gain margin are very large. The bode plots for LCL-T SPRC are drawn from the state space model Eqs. (7) and (8). The frequency response of the LCL-T SPRC is shown in Fig. 15. It clearly shows that the LCL-T converter is stable, the phase margin is about 35°, and the gain margin is approximately 17 dB.

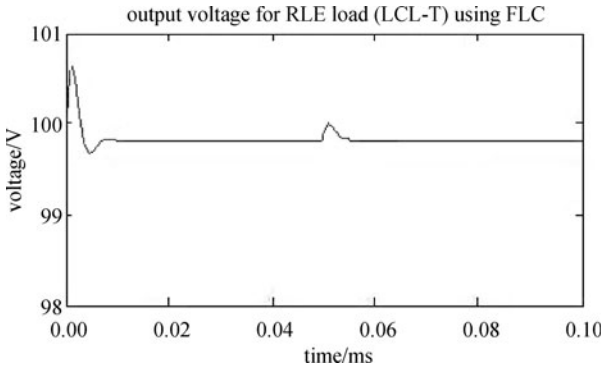

Fig. 12 Output voltage for step change in supply at t = 0.05 ms

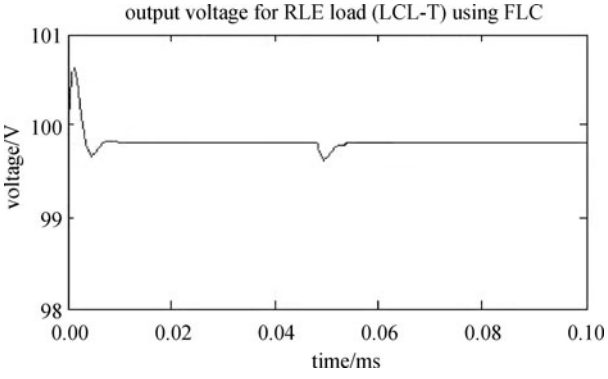

Fig. 13 Output voltage for step change in load at t = 0.05 ms

5 Experimental results

A prototype SPRC that was operated at 300 W, 100 kHz was designed. The output voltage of the SPRC changes with the change in load and supply. To regulate the output voltage of proposed converter, a closed-loop control system is designed and implemented. TMS320F2407 DSP is used to generate driving pulses, these pulses are amplified using the driver IC IR2110. The pulses are

Table 2 Comparative evaluation of transient and steady-state performances by using FLC

resonant topologies	settling time/ms	overshoot%	steady-state error/V
LCL-T	0.01	1	0.001
LLC-T	0.025	3	0.004

applied to the gate of the IRF840 MOSFETs through the opto coupler 6N137 and driver IRF 2N2112. The diodes MUR 4100 are used for the output bridge rectifier. The fuzzy controlling program is implemented by this DSP. The resonant voltage and current for LLC-T SPRC are shown in Fig. 16. It clearly shows that inverter output voltage and current are not in phase because harmonics present in the resonant tank. The output voltage with load and supply disturbance with t = 0.05 ms is presented in Fig. 17.

The above figures show the fuzzy controller output signal for this test. These figures show the good dynamic performance of the controller. It is clearly seen from the above figures that the resonant voltage, resonant current, and output voltage contain harmonic, and this harmonic effect is relatively hard for the whole circuit because nonlinear loads affect the resonant circuit.

Figures 18 and 19 present the inverter voltage, inverter current, and output voltage with disturbance for LCL-T SPRC, which are measured from the point A and B of the bridge inverter.

It can be seen from Fig. 18 that the current contains low harmonic and it presents a nearly sinusoidal shape. The controller shows a good performance of the whole design. It can be concluded that the controller is capable of operating under load-independent operation; again, it can be seen that the output follows the reference with good accuracy and better dynamic performances.

The LCL-T SPRC and LLC-T SPRC are verified by simulation and experimental studies. The performance shown in Table 3 proved that the control characteristics of the experimental results are observed to closely match the theoretical values, and the output voltage is seen to be nearly independent of load.

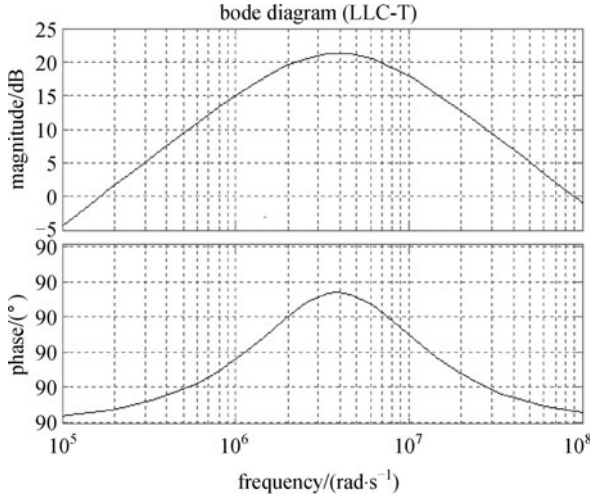

Fig. 14 Frequency response of LLC-T SPRC

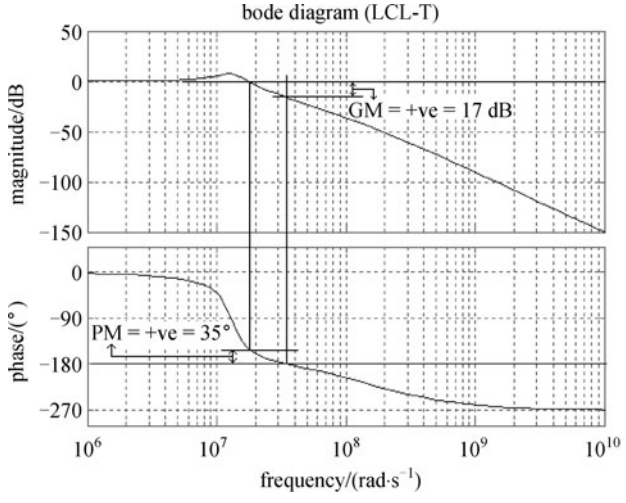

Fig. 15 Frequency response of LCL-T SPRC

Fig. 16 CH1: resonant voltage [volt scale: 40 V/div], CH2: resonant current [ampere scale: 0.5 A/div] for LLC-T SPRC

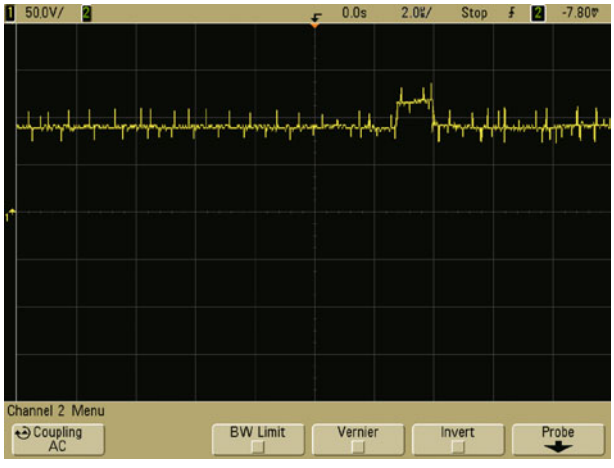

Fig. 17 Output voltage for LLC-T SPRC with load and supply disturbance at t = 0.05 ms (CH1: volt scale: 50 V/div)

Fig. 18 CH1: resonant voltage [volt scale: 40 V/div]. CH2: resonant current [ampere scale: 0.5 A/div] for LCL-T SPRC

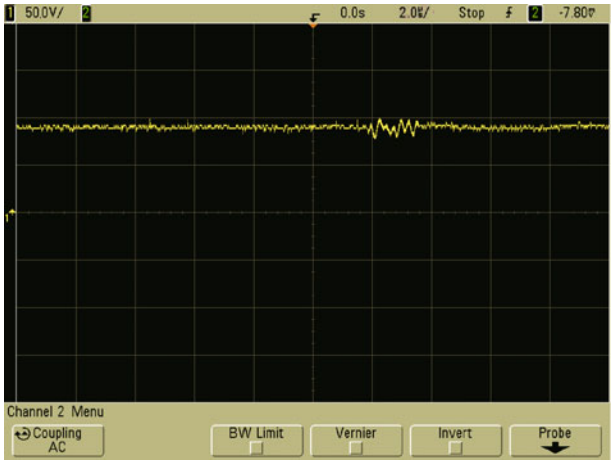

Fig. 19 Output voltage for LCL-T SPRC with load and supply disturbance at t = 0.05 ms (CH1: volt scale: 50 V/div)

Table 3 Performance measures of theoretical and simulation results

resonant topologies	load disturbance				supply disturbance			
	simulation studies		experimental studies		simulation studies		experimental studies	
	settling time/ms	overshoot/%	settling time/ms	overshoot/%	settling time/ms	overshoot/%	settling time/ms	overshoot/%
LLC-T SPRC	0.04	0.16	0.3	0.75	0.032	0.15	0.6	1
LCL-T SPRC	0.025	1	0.2	0.9	0.025	0.09	0.1	0.8

6 Conclusion

The stability analysis of SPRC has been modeled and simulated for estimating the performance for various load conditions. It has been found from the simulated results that the closed-loop controller provides better control strategies. It is concluded that the FLC based SPRC circuit provides load independent operation and better voltage regulation. A prototype 300 W, 100 kHz converter was designed. The experiment results are compared with the simulation results and the simulation results agree with the experimental results.

References

1. Raju G S N, Doradla S. An LCL resonant converter with PWM control-analysis, simulation, and implementation. IEEE Transactions on Power Electronics, 1995, 10(2): 164–174
2. Bhat A K S. Analysis and design of LCL-type series resonant converter. In: Proceedings of the 12th International Telecommunications Energy Conference (INTELEC'90). 1990, 172–178
3. Borage M, Tiwari S, Kotaiah S. LCL-T resonant converter with clamp diodes: A novel constant-current power supply with inherent constant-voltage limit. IEEE Transactions on Industrial Electronics, 2007, 54(2): 741–746
4. Borage M B, Nagesh K V, Bhatia M S, Tiwari S. Characteristics and design of an asymmetrical duty-cycle-controlled LCL-T resonant converter. IEEE Transactions on Power Electronics, 2009, 24(10): 2268–2275
5. Borage M, Tiwari S, Kotaiah S. Analysis and design of an LCL-T resonant converter as a constant-current power supply. IEEE Transactions on Industrial Electronics, 2005, 52(6): 1547–1554
6. Belaguli V, Bhat A K S. Series-parallel resonant converter operating in discontinuous current mode-analysis, design, simulation, and experimental results. IEEE Transactions on Circuits and Systems I: Fundamental Theory and Applications, 2000, 47(4): 433–442
7. Mattavelli P, Rossetto L, Spiazzi G, Tenti P, General-purpose fuzzy controller for DC-DC converters. IEEE Transactions on Power Electronics, 1997, 12(1): 79–86
8. Correa J M, Hutto E D, Farret F A, Simoes M G. A fuzzy-controlled pulse density modulation strategy for a series resonant inverter with wide load range. In: Proceedings of the 34th IEEE Annual Power Electronics Specialist Conference. 2003, 4: 1650–1655
9. Lakshminarasamma N, Masihuzzaman M, Ramanarayanan V. Steady state stability of current mode active clamp ZVS DC-DC converter. IEEE Transactions on Power Electronics, 2010, 25(6): 1546–1555
10. Arun S, Rama Raddy S. PSPICE simulation and implementation of closed loop controlled ZVS LCL push-pull DC-DC converter. International Journal of Computer Science and Network Security, 2008, 8(6): 67–73
11. Foster M P, Gould C R, Gilbert A J, Stone D A, Bingham C M. Analysis of CLL voltage-output resonant converters using describing function. IEEE Transactions on Power Electronics, 2008, 23(4): 1772–1781

12. Sivakumaran T S, Natarajan S P. Development of fuzzy control of series-parallel loaded resonant converter-simulation and experimental evaluation. In: Proceedings of India International Conference on Power Electronics. 2006, 360–364
13. Arulselvi S, Govindarajan U, Saminath V. Development of simple fuzzy logic controller (SFLC) for ZVS quasi-resonant converter: Design, simulation and experimentation. Journal of the Indian Institute of Science, 2006, 86: 215–233
14. Arulselvi S, Uma G, Chidambaram M. Design of PID controller for boost converter with RHS zero. In: Proceedings of the 4th International Conference on Power Electronics and Motion Control. 2004, 2: 532–537
15. Kaithamalai U, Ponnusamy L, Kandasamy B. Hybrid posicast controller for a DC-DC buck converter. Serbian Journal of Electrical Engineering, 2008, 5(1): 121–138
16. Nagarajan C, Madheswaran M. Performance analysis of LCL-T resonant converter with fuzzy/PID using state space analysis. Electrical Engineering, 2011, 93(3): 167–178
17. Nagarajan C, Madheswaran M. Stability analysis of series parallel resonant converter with fuzzy logic controller using state space techniques. Electric Power Components and Systems, 2011, 39(8): 780–793